

Photoinduced Energy Transfer in a Conformationally Flexible Re(I)/Ru(II) Dyad Probed by Time-Resolved Infrared Spectroscopy: Effects of Conformation and Spatial Localization of Excited States

Timothy L. Easun,[†] Wassim Z. Alsindi,[‡] Michael Towrie,[§] Kate L. Ronayne,[§] Xue-Zhong Sun,[‡] Michael D. Ward,^{*†} and Michael W. George^{*‡}

Department of Chemistry, University of Sheffield, Sheffield S3 7HF, U.K., School of Chemistry, University of Nottingham, University Park, Nottingham NG7 2RD, U.K., and Central Laser Facility, Science and Technology Facilities Council, Rutherford Appleton Laboratory, Harwell Science and Innovation Campus, Didcot OX11 0QX, U.K.

Received October 10, 2007

The dyad **RuLRe** contains {Re(bpy)(CO)₃Cl} and {Ru(bpy)(bpyam)₂}²⁺ termini (bpy = 2,2'-bipyridine; bpyam = 4,4'-diethylamido-2,2'-bipyridine) separated by a flexible ethylene spacer. Luminescence studies reveal the expected Re → Ru photoinduced energy transfer, with partial quenching of Re^I-based triplet metal-to-ligand charge-transfer (³MLCT) luminescence and consequent sensitization of the Ru^{II}-based ³MLCT luminescence, which has a component with a grow-in lifetime of 0.76 (±0.2) ns. The presence of IR-active spectroscopic handles on both termini [CO ligands directly attached to Re^I and amide carbonyl substituents on the bpy ligands coordinated to Ru^{II}] allowed the excited-state dynamics to be studied by time-resolved IR (TRIR) spectroscopy in much more detail than allowed by luminescence methods. A combination of picosecond- and nanosecond-time-scale TRIR studies revealed the presence of at least three distinct Re → Ru energy-transfer processes, with lifetimes of ca. 20 ps and 1 and 13 ns. This complex behavior occurs because of a combination of two different Ru-based ³MLCT states (Ru → L and Ru → bpyam), which are sensitized by energy transfer from the Re^I donor at different rates; and the presence of at least two conformers of the flexible molecule **RuLRe**, which have different Re...Ru separations.

Introduction

Photoinduced energy transfer (PEnT) between metal complex units across a range of bridging ligands has been extensively studied¹ because of its relevance to naturally occurring processes in photosynthesis and its importance in

a wide range of applications including solar energy harvesting,² artificial light-driven molecular devices,³ sensing and imaging,⁴ and display devices.⁵ It is now well-known that the energy-transfer process can occur by one of two mechanisms (Förster⁶ or Dexter⁷), such that the bridging

* To whom correspondence should be addressed. E-mail: m.d.ward@sheffield.ac.uk (M.D.W.), mike.george@nott.ac.uk (M.W.G.).

[†] University of Sheffield.

[‡] University of Nottingham.

[§] Rutherford Appleton Laboratory, Harwell Science and Innovation Campus.

(1) For general reviews on energy transfer, see: (a) Balzani, V.; Juris, A.; Venturi, M.; Campagna, S.; Serroni, S. *Chem. Rev.* **1996**, *96*, 759. (b) Barigelletti, F.; Flamigni, L. *Chem. Soc. Rev.* **2000**, *29*, 1. (c) Ward, M. D. *Coord. Chem. Rev.* **2007**, *251*, 1663. (d) Balzani, V.; Bergamini, P.; Marchioni, F.; Ceroni, P. *Coord. Chem. Rev.* **2006**, *250*, 1245. (e) Scandola, F.; Chiorboli, C.; Prodi, A.; Iengo, E.; Alessio, E. *Coord. Chem. Rev.* **2006**, *250*, 1471. (f) Welter, S.; Salluce, N.; Belsler, P.; Groeneveld, M.; De Cola, L. *Coord. Chem. Rev.* **2005**, *249*, 1360. (g) Huynh, M. H. V.; Dattelbaum, D. M.; Meyer, T. J. *Coord. Chem. Rev.* **2005**, *249*, 457. (h) Nakamura, Y.; Aratani, N.; Osuka, A. *Chem. Soc. Rev.* **2007**, *36*, 831. (i) Ward, M. D. *Chem. Soc. Rev.* **1997**, *26*, 365.

(2) (a) Noy, D. *Photosynth. Res.* **2008**, *95*, 23. (b) Katterle, M.; Prokhorenko, V. I.; Holzwarth, A. R.; Jesorka, A. *Chem. Phys. Lett.* **2007**, *447*, 284. (c) Scully, S. R.; Armstrong, P. B.; Edder, C.; Frechet, J. M. J.; McGehee, M. D. *Adv. Mater.* **2007**, *19*, 2961. (d) Balaban, T. S.; Berova, N.; Drain, C. M.; Hauschild, R.; Huang, X.; Kalt, H.; Lebedkin, S.; Lehn, J.-M.; Nifaitis, F.; Pescitelli, G.; Prokhorenko, V. I.; Riedel, G.; Smeureanu, G.; Zeller, J. *Chem.—Eur. J.* **2007**, *13*, 8411. (e) Siegers, C.; Hohl-Ebinger, J.; Zimmernann, B.; Würfel, U.; Mulhaupt, R.; Hinsch, A.; Haag, R. *ChemPhysChem* **2007**, *8*, 1548. (f) Polivka, T.; Pellnor, M.; Melo, E.; Pascher, T.; Sundstrom, V.; Osuka, A.; Naqvi, K. R. *J. Phys. Chem.* **2007**, *111*, 467.

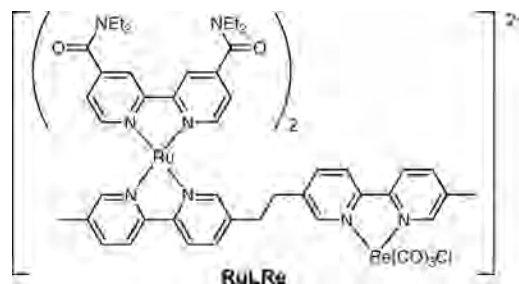
(3) (a) Baranoff, E.; Barigelletti, F.; Bonnet, S.; Collin, J.-P.; Flamigni, L.; Mobian, P.; Sauvage, J.-P. *Struct. Bonding (Berlin)* **2007**, *123*, 41. (b) Bonnet, S.; Collin, J.-P.; Koizumi, M.; Mobian, P.; Sauvage, J.-P. *Adv. Mater.* **2006**, *18*, 1239. (c) Credi, A. *Aust. J. Chem.* **2006**, *59*, 157. (d) Li, Y.-J.; Li, H.; Li, Y.-L.; Liu, H.-B.; Wang, S.; He, X.-R.; Wang, N.; Zhu, D.-B. *Org. Lett.* **2005**, *7*, 4835. (e) Jukes, R. T. F.; Adamo, V.; Hartl, F.; Belsler, P.; De Cola, L. *Coord. Chem. Rev.* **2005**, *249*, 1327.

ligand plays an important role not only in controlling the intercomponent distance, to which both mechanisms are sensitive, but also in determining the magnitude of metal–metal electronic coupling, which is relevant to Dexter energy transfer.⁷

Most commonly, PEnT is probed by luminescence methods. If both donor and acceptor components are luminescent, then the rate of energy transfer can be determined from either the reduced emission lifetime of the energy donor unit or the rise time in the sensitized luminescence of the acceptor unit or both.¹ However, if dark (nonluminescent) states are involved, then time-resolved infrared (TRIR) spectroscopy, which measures changes in the stretching vibration frequency of IR-active functional groups when the excited state is formed, can be used.^{8–10} This technique has the additional advantage that it can operate on very short time scales (picoseconds) such that processes that are too fast to detect by luminescence methods can readily be observed by TRIR.

In this paper, we describe the synthesis and photophysical study of the dinuclear complex **RuLRe**, comprising a {Re(CO)₃Cl(bpy)} terminus (hereafter **Re-CO**) connected by a flexible saturated ethylene spacer to a {Ru(bpy)(bpyam)}²⁺ (bpyam = 4,4'-diethylamido-2,2'-bipyridine) terminus (hereafter **Ru-bpy**), via use of the bis-bipyridyl ligand **L** as the bridging group. The mononuclear complexes [Ru(bpyam)₂-L]²⁺ (**RuL**) and [Re(CO)₃Cl(bpy)] [**Re(bpy)**] were also investigated as model complexes for comparison. TRIR studies on this dyad and the mononuclear model complexes have allowed us to monitor the intercomponent Re → Ru energy-transfer process^{10,11} and show how it is related to

the conformation of the molecule in much more detail than is possible from luminescence measurements.



Results and Discussion

Design and Synthesis of the Dyad. TRIR spectroscopy requires an IR-active functional group to act as a spectroscopic “handle” on each component.^{8–10} Ideally, these groups should have a vibration in a region free from interference by solvent and fingerprint bands, i.e., 1600–2200 cm⁻¹; they should undergo an easily measurable shift when the electron distribution changes following the formation of an excited state and, in a dyad, ideally they should not overlap with each other such that two distinct sets of signals, one belonging to each component, can be identified. For PEnT to occur, the dyad needs to contain two components of which one has a significantly higher excited-state energy than the other, providing the necessary gradient, and the lifetime of the donor must be long enough such that the energy-transfer rate is faster than the intrinsic deactivation rate by luminescence, which also means that the separation between components should be less than the critical radius for energy transfer if Förster energy transfer is involved.⁶

These criteria led us to the complex **RuLRe**. Both rhenium(I)¹² and ruthenium(II)¹³ bipyridyl complexes have long-lived (tens/hundreds of nanoseconds) luminescent triplet metal-to-ligand charge-transfer (³MLCT) excited states. The carbonyl ligands at the Re^I center and the amide carbonyl substituents on the bipyridyl ligands at the Ru^{II} center show substantial shifts of their vibrational frequencies in the excited state and are far enough apart to be unambiguously assigned in the IR spectrum.⁸ The lowest ³MLCT excited state of Re^I complexes of this type is well-known to lie significantly above that of ruthenium(II) bipyridyl complexes such that Re^I → Ru^{II} PEnT occurs as long as the bridging ligand is

- (4) (a) Duong, H. D.; Il Rhee, J. *Talanta* **2007**, *73*, 899. (b) Komatsu, K.; Urano, Y.; Kojima, H.; Nagano, T. *J. Am. Chem. Soc.* **2007**, *129*, 13447. (c) Lay, T. J.; Griesbeck, O.; Yue, D. T. *Biophys. J.* **2007**, *93*, 4031. (d) Ben Othman, A.; Lee, J. W.; Wu, J. S.; Kim, J. S.; Abidi, R.; Thuery, P.; Strub, J. M.; Van Dorsselaer, A.; Vicens, J. *J. Org. Chem.* **2007**, *72*, 7634. (e) Finikova, O. S.; Troxler, T.; Senes, A.; DeGrado, W. F.; Hochstrasser, R. M.; Vinogradov, S. A. *J. Phys. Chem. A* **2007**, *111*, 6977. (f) Coskun, A.; Deniz, E.; Akkaya, E. U. *Tetrahedron Lett.* **2007**, *48*, 5359. (g) De, A.; Loening, A. M.; Gambhir, S. S. *Cancer Res.* **2007**, *67*, 7175. (h) Bogner, M.; Ludewig, U. *J. Fluorescence* **2007**, *17*, 350. (i) Plush, S. E.; Gunnlaugsson, T. *Org. Lett.* **2007**, *9*, 1919. (j) Kim, J. S.; Choi, M. G.; Song, K. C.; No, K. T.; Ahn, S.; Chang, S. K. *Org. Lett.* **2007**, *9*, 1129.
- (5) (a) Evans, R. C.; Douglas, P.; Winscom, C. K. *Coord. Chem. Rev.* **2006**, *150*, 2093. (b) Bansal, A. K.; Penzkofer, A.; Holzer, W.; Tsuboi, T. *Mol. Cryst. Liq. Cryst.* **2007**, *467*, 21. (c) Montes, V. A.; Perez-Bolivar, C.; Agarwal, N.; Shinar, J.; Anzenbacher, P. *J. Am. Chem. Soc.* **2006**, *128*, 12436. (d) Tsuzuki, T.; Makayama, Y.; Nakamura, J.; Iwata, T.; Tokito, S. *Appl. Phys. Lett.* **2006**, *88*, 243511. (e) Lundin, N. J.; Blackman, A. G.; Gordon, K. C.; Officer, D. L. *Angew. Chem., Int. Ed.* **2006**, *45*, 2582. (f) Coppo, P.; Duati, M.; Kozhevnikov, V. N.; Hofstraat, J. W.; De Cola, L. *Angew. Chem., Int. Ed.* **2005**, *44*, 1806.
- (6) Förster, Th. H. *Discuss. Faraday Soc.* **1959**, *27*, 7.
- (7) Dexter, D. L. *J. Chem. Phys.* **1953**, *21*, 836.
- (8) Butler, J. M.; George, M. W.; Schoonover, J. R.; Dattelbaum, D. M.; Meyer, T. J. *Coord. Chem. Rev.* **2007**, *251*, 492.
- (9) Alsindi, W. Z.; Easun, T. L.; Sun, X.-Z.; Ronayne, K. L.; Towrie, M.; Herrera, J.-M.; George, M. W.; Ward, M. D. *Inorg. Chem.* **2007**, *46*, 3696.
- (10) (a) Schoonover, J. R.; Gordon, K. C.; Argazzi, R.; Woodruff, W. H.; Peterson, K. A.; Bignozzi, C. A.; Dyer, R. B.; Meyer, T. J. *J. Am. Chem. Soc.* **1993**, *115*, 10996. (b) Schoonover, J. R.; Shreve, A.; Dyer, R. B.; Cleary, R. L.; Ward, M. D.; Bignozzi, C. A. *Inorg. Chem.* **1998**, *37*, 2598.

- (11) (a) Lazarides, T.; Barbieri, A.; Sabatini, C.; Barigelletti, F.; Adams, H.; Ward, M. D. *Inorg. Chim. Acta* **2007**, *360*, 814. (b) Furue, M.; Naiki, M.; Kanematsu, Y.; Kushida, T.; Kamachi, M. *Coord. Chem. Rev.* **1991**, *111*, 221. (c) van Wallendaal, S.; Perkovic, M. W.; Rillema, D. P. *Inorg. Chim. Acta* **1993**, *213*, 253. (d) Bardwell, D. A.; Barigelletti, F.; Cleary, R. L.; Flamigni, L.; Guardigli, M.; Jeffery, J. C.; Ward, M. D. *Inorg. Chem.* **1995**, *33*, 2438. (e) Cleary, R. L.; Byrom, K. J.; Bardwell, D. J.; Jeffery, J. C.; Ward, M. D.; Calogero, G.; Armaroli, N.; Flamigni, L.; Barigelletti, F. *Inorg. Chem.* **1997**, *36*, 2601.
- (12) (a) Schanze, S. K.; MacQueen, D. B.; Perkins, T. A.; Cabana, L. A. *Coord. Chem. Rev.* **1993**, *122*, 63. (b) Worl, L. A.; Duesing, R.; Chen, P.; Della Ciana, L.; Meyer, T. J. *J. Chem. Soc., Dalton Trans.* **1991**, 849. (c) Sacksteder, L.; Lee, M.; Demas, J. N.; DeGraff, B. A. *J. Am. Chem. Soc.* **1993**, *115*, 8230.
- (13) (a) Meyer, T. J. *Pure Appl. Chem.* **1986**, *58*, 1193. (b) Juris, A.; Balzani, V.; Barigelletti, F.; Campagna, S.; Belser, P.; von Zelewsky, A. *Coord. Chem. Rev.* **1988**, *84*, 85.

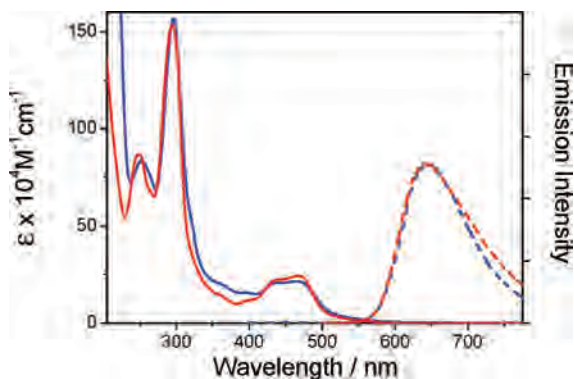


Figure 1. UV/vis absorption spectra (solid lines) and emission spectra (dashed lines; $\lambda_{\text{ex}} = 405$ nm) of **RuL** (red) and **RuLRe** (blue) at room temperature in CH_3CN .

reasonably short (see below).^{10,11} Finally, the saturated spacer means that the Ru^{II} and Re^I chromophores are electronically isolated such that their individual properties can be estimated very closely using appropriate mononuclear model complexes.

Synthesis of **RuLRe** was straightforward by the stepwise attachment of $\{\text{Ru}(\text{bpyam})_2\}^{2+}$ and then $\{\text{Re}(\text{CO})_3\text{Cl}\}$ fragments to the bipyridyl sites of L. The intermediate mononuclear complex $[\text{Ru}(\text{bpyam})_2\text{L}]^{2+}$ (**RuL**) has been reported by us recently;¹⁴ reaction of this with $\text{Re}(\text{CO})_5\text{Cl}$ allowed the formation of **RuLRe**, which was isolated as its bischloride salt, in moderate yield. The complex was satisfactorily characterized by a combination of elemental analysis and MALDI mass spectrometry, and the IR spectrum in CH_3CN showed the presence of the amide carbonyl substituents attached to the bpy ligands at the Ru^{II} terminus at 1636 cm^{-1} and the three CO ligands coordinated to the Re^I terminus in the region $1898\text{--}2024\text{ cm}^{-1}$.

UV/Vis Absorption and Luminescence Properties. The absorption spectrum of **RuLRe** in CH_3CN displays absorption features characteristic of both mononuclear complexes **RuL** and **Re-bpy** (Figure 1). In particular, the strong singlet metal-to-ligand charge-transfer (¹MLCT) absorptions between 400 and 500 nm characteristic of the Ru^{II} terminus are clearly visible in the spectrum of **RuLRe**; the weaker, higher energy ¹MLCT absorption characteristic of the Re^I terminus is apparent as a region of increased absorbance in the 350–400 nm region.¹² This absorption spectrum is typical of Ru–Re dyads of this type.^{11a–d}

Excitation into any of these absorption bands in **RuLRe** results in a broad emission at 645 nm. This is very similar in energy, intensity, and lifetime to the emission obtained from the mononuclear complex **RuL** at ca. 641 nm,¹⁴ which is associated with a Ru \rightarrow bpyam ³MLCT state because the bpyam ligands have a lower-lying lowest unoccupied molecular orbital than the bpy fragment of the bridging ligand L.¹⁵ This Ru-based luminescence is, however, significantly different from the shorter-lived and weaker emission of

Re-bpy at ca. 618 nm.^{12b} The luminescence lifetimes were obtained using 405 nm excitation, a wavelength where the two chromophores are excited in a ca. 1:0.3 ratio (Ru/Re; Table 1). The emission lifetime of **RuLRe** was determined at 10 nm intervals between 570 and 680 nm, and at all wavelengths, the emission contained at least two decays; fitting these data to a biexponential function consistently gave one short ($\tau = 10\text{--}35$ ns) and one long ($\tau = 280\text{--}305$ ns) luminescence component.¹⁶

Although the emission spectrum shows a maximum at 645 nm, analysis of the lifetime data, using the relative contributions of each lifetime component of the biexponential decay (using $\tau_1 = 20$ ns and $\tau_2 = 295$ ns) at each wavelength, revealed that there were two emission bands with peak maxima at 645 nm (major component, ca. 86%) and 620 nm (minor component, ca. 14%). The weak band at 620 nm can be compared to the analogous mononuclear **Re-bpy** complex (emission at 618 nm;^{12b} $\tau = 31$ ns), and this shorter decay component from **RuLRe** can therefore be assigned to Re-based emission. The fact that residual Re-based emission can be detected from **RuLRe** means that Re \rightarrow Ru energy transfer is incomplete, although the occurrence of partial Re \rightarrow Ru energy transfer may be inferred from the reduction of the Re-based emission lifetime from 31 ns in **Re-bpy** to ca. 20 ns in **RuLRe**. The occurrence of Re \rightarrow Ru energy transfer is further confirmed by the fact that the 645 nm emission component of **RuLRe** has a grow-in (rise time) of 0.76 (± 0.2) ns, characteristic of sensitized emission following energy transfer, which occurs with a rate constant of $1.3 \times 10^9\text{ s}^{-1}$ (the reciprocal of the rise time).

Recording the emission spectrum of **RuL** at 77 K in an EtOH/MeOH (4:1) glass directly yields the ³MLCT energy of the emissive state as $16\,585\text{ cm}^{-1}$ (from emission at 603 nm) which is some 1935 cm^{-1} lower in energy than the ³MLCT energy of **Re-bpy** at $18\,520\text{ cm}^{-1}$ (from 77 K emission in methyltetrahydrofuran at 540 nm^{12b}). The absorption maxima of **RuLRe** can be used to estimate the relative energies of the ¹MLCT states in the dyad: the lowest-energy peak maximum, corresponding to the Ru \rightarrow bpyam state, is at 475 nm; the Ru \rightarrow L state is ca. 1936 cm^{-1} higher in energy at 435 nm, and the Re \rightarrow L excited state is a further 4039 cm^{-1} higher in energy at 368 nm. Assuming that this relative energy level ordering is maintained in the ³MLCT excited states of **RuLRe**, we can use the model complexes to estimate the energy of the Ru \rightarrow bpyam ³MLCT state as ca. $16\,600\text{ cm}^{-1}$; the energy of the Ru \rightarrow L ³MLCT state is ca. $17\,200\text{ cm}^{-1}$, and the energy of the Re \rightarrow L ³MLCT state is ca. $18\,500\text{ cm}^{-1}$.

TRIR Studies. (i) Picosecond-Time-Scale Experiments. In order to probe the energy-transfer process in more detail and with better time resolution, we have examined the photo-physics of **RuLRe** further using TRIR spectroscopy. The picosecond TRIR spectra in the metal–carbonyl region of **RuLRe** in CH_3CN , following 400 nm excitation into the ¹MLCT absorption manifold, are shown in Figure 2. It is

(14) Lazarides, T.; Easun, T. L.; Veyne-Marti, C.; Alsindi, W. Z.; George, M. W.; Deppermann, N.; Hunter, C. A.; Adams, H.; Ward, M. D. *J. Am. Chem. Soc.* **2007**, *129*, 4014.

(15) Omberg, K. M.; Smith, G. D.; Kavaliunas, D. A.; Chen, P.-Y.; Treadway, J. A.; Schoonover, J. R.; Palmer, R. A.; Meyer, T. J. *Inorg. Chem.* **1999**, *38*, 951.

(16) This does not preclude the possibility that there could be more unresolved components, but, nonetheless, a satisfactory fit could be obtained using only two in each case.

Table 1. UV/Vis Spectroscopic and Photophysical Data^a

complex	absorption $\lambda_{\text{max}}/\text{nm}$ ($10^{-3}\epsilon \text{ M}^{-1} \text{ cm}^{-1}$)				emission ^b		
					$\lambda_{\text{max}}/\text{nm}$	$10^2\phi^c$	τ (ns)
RuL	300 (143.3)	367 (13.0)	432 (21.6)	471 (24.1)	641	4.1	341 \pm 10
Re-bpy ^{12b}		370 (2.5)			618	0.3	31
RuLRe	295 (156.8)	368 (18.8)	396 (15.7)	435 (20.7)	645	<i>d</i>	20 (\pm 2), 295 (\pm 6)

^a Measured in air-equilibrated CH₃CN at room temperature. Sample concentrations were $1 \times 10^{-5} \text{ M}$. ^b Excitation wavelength = 405 nm. The emission maxima and quantum yields ($\pm 10\%$) are from corrected spectra. ^c Measured against a [Ru(bpy)₃]Cl₂ standard solution in H₂O ($\phi = 0.028$). ^d The quantum yield varies with the excitation wavelength; see the text.

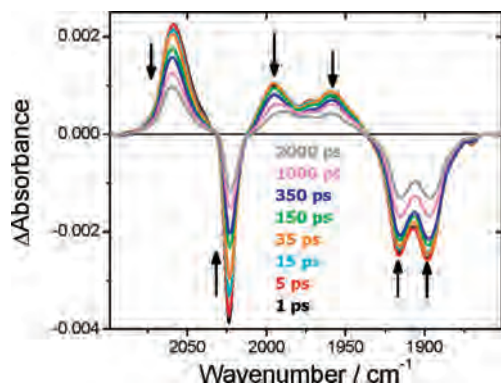


Figure 2. Picosecond-TRIR difference spectra of **RuLRe** in CH₃CN in the rhenium carbonyl region with $\lambda_{\text{ex}} = 400 \text{ nm}$. Selected time delays after laser excitation are as shown.

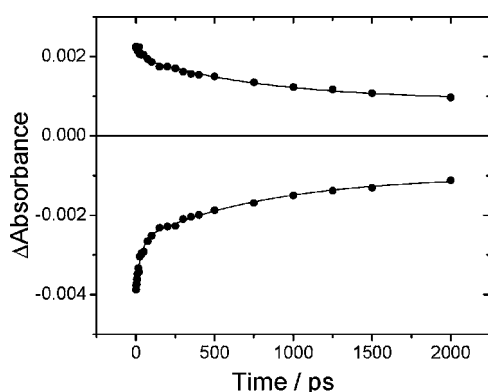


Figure 3. Kinetics of the parent bleach at 2024 cm^{-1} (bottom) and the transient band at 2059 cm^{-1} (top) of **RuLRe** in CH₃CN after laser excitation at 400 nm . The data can be fitted to a biexponential decay of 22 and 830 ps (solid lines).¹²

clear that the $\nu(\text{CO})$ bands of the $\text{Re}(\text{CO})_3$ moiety (1898 , 1916 , and 2024 cm^{-1}) are bleached, and new bands to higher wavenumber (1959 , 1995 , and 2059 cm^{-1}) characteristic of a $\text{Re} \rightarrow \text{bpy}^3\text{MLCT}$ excited state are produced, in which the Re^{I} center is transiently oxidized and the CO bonds are thereby strengthened. The shifts in $\nu(\text{CO})$ are entirely typical of $^3\text{MLCT}$ states.¹⁰ These bands decay synchronously with the recovery of the parent $\nu(\text{CO})$ bands, and fitting these data to two exponentials affords lifetimes of $22 (\pm 10)$ and $830 (\pm 200)$ ps (Figure 3) for the Re-based $^3\text{MLCT}$ state.¹⁶

We have also monitored the amide CO band in order to probe the **RuL** component of **RuLRe**. The parent band bleach at 1636 cm^{-1} is formed by the initial laser flash and persists on the time scale of the measurement ($1-2 \text{ ns}$). The TRIR spectrum obtained 2 ps after the laser flash shows that, following 400 nm excitation, the $\nu(\text{CO})_{\text{amide}}$ band shifts to

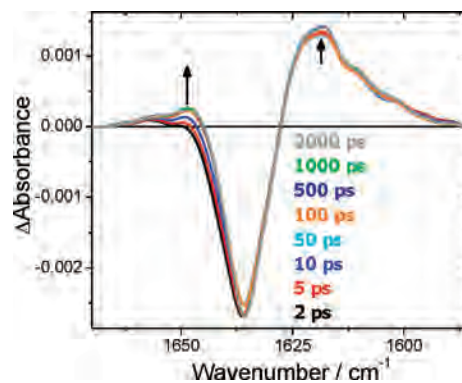


Figure 4. Picosecond-TRIR difference spectra of **RuLRe** in CH₃CN in the amide carbonyl region with $\lambda_{\text{ex}} = 400 \text{ nm}$. Selected time delays after laser excitation are as shown.

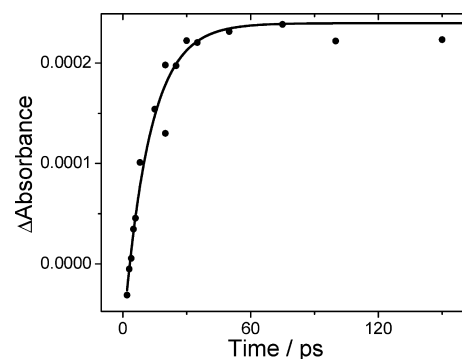


Figure 5. Early time kinetics of the transient band at 1649 cm^{-1} of **RuLRe** in CH₃CN after laser excitation at 400 nm . The data can be fitted to a growth of 13 ps (solid line).

lower energy (1619 cm^{-1} ; Figure 4). This transient band is typical of the formation of the $\text{Ru} \rightarrow \text{bpyam}^3\text{MLCT}$ excited state in which a bpyam ligand is transiently reduced.⁹ After the initial subpicosecond formation, this low-energy transient band continues to increase in magnitude with $\tau = 750 (\pm 400)$ ps, indicative of the grow-in of the Ru-based excited state that we also observed by luminescence methods. This grow-in rate also correlates well with the slower of the two decay components of the Re-based $^3\text{MLCT}$ state [$830 (\pm 200)$ ps] that we observed on the picosecond time scale.

There is also a weak transient band at 1649 cm^{-1} , higher in energy than the $\nu(\text{CO})_{\text{amide}}$ parent band at 1636 cm^{-1} , which grows with $\tau = 13 (\pm 5)$ ps (Figure 5) and then persists for the duration of the measurement ($1-2 \text{ ns}$). The formation of a band at higher wavenumber than the parent is consistent with the formation of an alternative Ru-based $^3\text{MLCT}$ excited state in which the excited electron resides on the coordinated bpy fragment of the bridging ligand rather than on a bpyam

ligand; i.e., a Ru → L ³MLCT state is populated in addition to the Ru → bpyam ³MLCT state. In this case, the transient oxidation of the Ru^{II} center results in a shift of the “spectating” ν(CO)_{amide} band on the bpyam ligands to higher energy.⁹ The grow-in of this Ru → L ³MLCT state [13 (±5) ps] correlates well with the fastest decay component of the Re-based ³MLCT state [22 (±10) ps].

Thus, on the basis of the picosecond-time-scale experiments, there appear to be two processes occurring. The faster decay of the Re → bpy ³MLCT state correlates with the growth of the Ru → L ³MLCT state that involves the bridging ligand at the Ru^{II} center. The slower decay of the Re → bpy ³MLCT state correlates with the increase in the population of the Ru → bpyam ³MLCT state. This could possibly be a result of the greater donor–acceptor distance between the Re energy-donor unit and the Ru → bpyam energy-acceptor unit, than between the Re energy-donor unit and the Ru → L energy-acceptor unit; or alternatively due to two different conformers being present in the solution, affording different energy-transfer rates.

The Ru → L ³MLCT state is expected to decay into the Ru → bpyam ³MLCT state on a subnanosecond time scale. Unfortunately, the kinetic data between 500 ps and 2 ns are not currently of sufficiently high quality in order to determine unambiguously the kinetics of this process. The growth of the lower energy ν(CO)_{amide} transient band of the Ru → bpyam ³MLCT state could be fitted to a biexponential rise as opposed to the monoexponential fit above, with both lifetimes ca. 800 ps, but this does not constitute direct evidence for the internal conversion of the Ru → L ³MLCT state. The persistence of the higher energy ν(CO)_{amide} transient band for at least 1 ns without significant decay may indicate the presence of another energy-transfer process “feeding” it from the Re → L excited state, on a time-scale commensurate with its decay by internal conversion. The occurrence of multiple rates of energy transfer involving a single ruthenium(II) polypyridine type chromophore, according to which of the ligands is involved in the ³MLCT state and its spatial relationship to other components in the assembly, has been observed in other cases.¹⁷

(ii) Nanosecond-Time-Scale Experiments. The decay of the Re-based MLCT state can be further monitored on the nanosecond time scale. Figure 6 shows the TRIR spectra obtained following 355 nm excitation of **RuLRe** in CH₃CN. The Re → L ³MLCT state is clearly visible on the nanosecond time scale, with the ν(CO)_{Re} bands of the excited state decaying biexponentially with time constants of ca. 1 and 13 (±3) ns at the same rate that the ground-state ν(CO)_{Re} band is completely reformed (Figure 7). The shorter component of ca. 1 ns is similar to the 830 (±200) ps component that was measured using picosecond-time-scale experiments (see above); the long-lived 13 (±3) ns component is, however, in addition to the picosecond-time-scale components and presumably correlates with the 20 ns Re-based

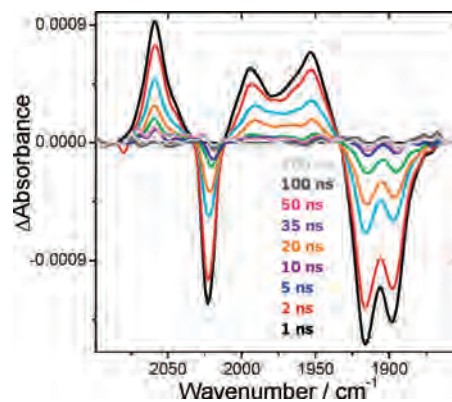


Figure 6. Nanosecond-TRIR difference spectra of **RuLRe** in CH₃CN in the rhenium carbonyl region with λ_{ex} = 355 nm. Selected time delays after laser excitation are as shown.

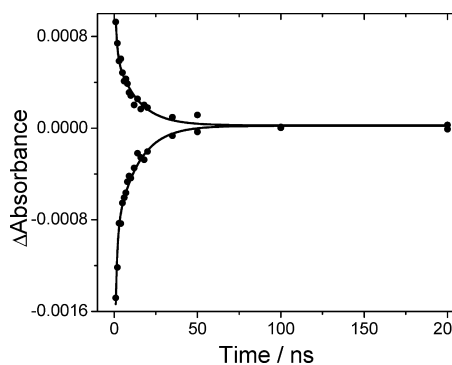


Figure 7. Kinetics of one parent bleach at 1918 cm⁻¹ (bottom) and the transient band at 2059 cm⁻¹ (top) of **RuLRe** in CH₃CN after laser excitation at 355 nm. The data can be fitted to a biexponential decay of 1 and 13 ns (solid lines).

luminescence component detected by the emission measurements. Note that the higher concentrations typically used for TRIR experiments compared to luminescence experiments result in reduced lifetimes due to a degree of self-quenching, such that lifetimes of 20 ns (by luminescence) and 13 (±3) ns (by TRIR) are consistent with the same excited-state decay process.

We have also monitored the amide carbonyl band in order to probe the **RuL** component of **RuLRe** on the longer nanosecond time scale. The Ru → bpyam ³MLCT excited state is apparent on this time scale (Figure 8), with the lower-energy ν(CO)_{amide} transient and parent bleach bands clearly present in the TRIR spectrum obtained 1 ns after photolysis. The weak higher-energy transient associated with the Ru → L ³MLCT state is not clearly observed after 1 ns. This may be due, in part, to the different excitation conditions between the two TRIR experiments (355 vs 400 nm excitation) and implies that the lifetime of this state is <1 ns. The lower-energy transient band continues to grow in over the first 20 ns, synchronously with further bleaching of the parent ν(CO)_{amide} band and on a similar time scale to the longer decay component [13 (±3) ns] of the Re → bpy ³MLCT state, indicative of a slow Re → Ru energy-transfer process. The parent and transient ν(CO)_{amide} bands of the Ru → bpyam ³MLCT state subsequently decay on a time scale of ca. 150 ns. This is shorter than the Ru-based lifetime obtained from

(17) (a) Constable, E. C.; Handel, R. W.; Housecroft, C. E.; Morales, A. F.; Flamigni, L.; Barigelli, F. *Dalton Trans.* **2003**, 1220. (b) Shavaleev, N. M.; Bell, Z. R.; Easun, T. L.; Rutkaite, R.; Swanson, L.; Ward, M. D. *Dalton Trans.* **2004**, 3678.

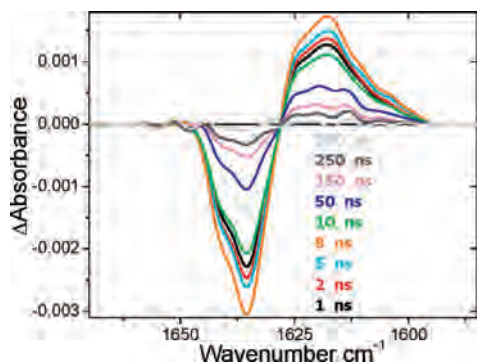


Figure 8. Nanosecond-TRIR difference spectra of **RuLRe** in CH_3CN in the amide carbonyl region with $\lambda_{\text{ex}} = 355 \text{ nm}$. Selected time delays after laser excitation are as shown.

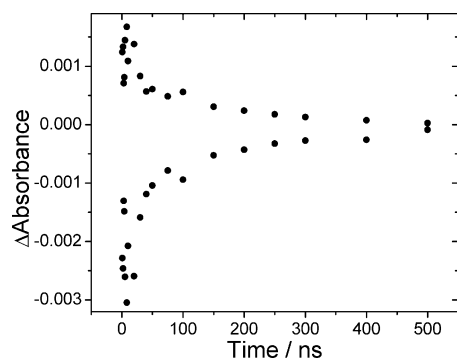


Figure 9. Kinetics of the parent bleach at 1635 cm^{-1} (bottom) and the transient band at 1619 cm^{-1} (top) of **RuLRe** in CH_3CN after laser excitation at 355 nm .

the emission experiments (295 ns) due to the higher concentration used in the TRIR experiments, as mentioned earlier.

It should be noted that the higher-energy nm excitation used for the nanosecond times-scale experiments would be expected to increase the initial relative proportion of the Re–L excited states to Ru-based excited states over that of 400 nm excitation. This change should not affect the energy-transfer rates observed and is expected to be small because comparison of the UV/vis absorption spectra of the model complexes indicates that the extinction coefficient of the **RuL** chromophore is still considerably higher than that of the **Re-bpy** chromophore at this wavelength.

Discussion of Results: Correlation of TRIR and Luminescence Behavior. The UV/vis and luminescence results clearly show that the predominant absorption and emission processes of **RuLRe** are Ru-based, with the Ru^{II} terminus hosting the lowest-energy $^3\text{MLCT}$ state from which most of the luminescence occurs following Re \rightarrow Ru energy transfer, which is itself in competition with the normal emission of the Re-based chromophore.

The combination of picosecond- and nanosecond-time-scale TRIR experiments shows that the Re \rightarrow L $^3\text{MLCT}$ excited state, which is the highest of the metal-based $^3\text{MLCT}$ states and acts as the energy donor for all Re \rightarrow Ru energy-transfer processes, decays with at least three time constants of $22 (\pm 10) \text{ ps}$, ca. 1 ns, and ca. 13 ns. The first of these corresponds to fast energy transfer to the Ru \rightarrow L $^3\text{MLCT}$

state based on the bridging ligand; this is not the lowest-energy Ru-based $^3\text{MLCT}$ state but is the one that is spatially closest to the Re center, with the two bpy fragments that are involved in the Re \rightarrow L and Ru \rightarrow L $^3\text{MLCT}$ states being part of the same bridging ligand and separated only by an ethylene bridge. The second and third of these Re-based decay components may *both* correspond to energy transfer from the Re \rightarrow L $^3\text{MLCT}$ state to the Ru \rightarrow bpyam $^3\text{MLCT}$ state, which occurs over a greater distance because the bpyam ligands are more remote from the Re^{I} center, and are therefore slower. The $\approx 1 \text{ ns}$ Re-based decay component is matched by corresponding grow-in in both the TRIR spectrum and the luminescence spectrum associated with the Ru \rightarrow bpyam $^3\text{MLCT}$ state. The 13 ns Re-based decay component is also matched by a grow-in of the corresponding Ru-based TRIR transient bands. In principle, we should also expect a 13 ns grow-in component to the Ru-based luminescence, but the overlap of Ru- and Re-based emission profiles, with several components in the same wavelength region (Re, $\approx 13 \text{ ns}$ decay; Ru, 1 ns grow-in and 295 ns decay), means that this additional expected 13 ns grow-in of the luminescence could not be deconvoluted. The behavior of both Re- and Ru-based signals on the nanosecond time scale is clearly observed by TRIR. The 13 ns decay component of the Re-based $^3\text{MLCT}$ state is also correlated with the observed weak Re-based luminescence and, together with the amount of quenching of the Re-based emission from the dyad compared with the mononuclear complex, suggests that the slowest energy-transfer process occurs on a time scale similar to that of emission, directly competing as a deactivation pathway of the Re-based $^3\text{MLCT}$ state.

The question arises as to why there should be two components, with lifetimes of ca. 1 and 13 ns, corresponding to PEnT from the Re \rightarrow L $^3\text{MLCT}$ state to the lowest-lying Ru \rightarrow bpyam $^3\text{MLCT}$ state. A plausible reason for this is the conformational flexibility of the molecule, which is not rigid but will exist as an ensemble of conformers with a range of $\text{Re}\cdots\text{Ru}$ separations.^{11a,18} The conformational flexibility of **RuLRe** has been estimated by undertaking simple molecular mechanics calculations, which show that the Ru–Re internuclear separation lies between the extremes of ca. 5.5 and 12.6 Å (Figure 10; see the Supporting Information for details).¹⁹ The different conformers will necessarily result in variable rates of energy transfer, and we suggest that the presence of both 1 and 13 ns components for Re \rightarrow Ru energy transfer involving the Ru \rightarrow bpyam $^3\text{MLCT}$ state as the lowest-energy acceptor is a consequence of the presence of two predominant conformers with short and long $\text{Re}\cdots\text{Ru}$ separations, respectively.

On this basis, we would also expect that there should also be at least two quite different rate constants for the energy

(18) (a) Pope, S. J. A.; Rice, C. R.; Ward, M. D.; Morales, A. F.; Accorsi, G.; Armaroli, N.; Barigelletti, F. *Dalton Trans.* **2001**, 2228. (b) Morales, A. F.; Accorsi, G.; Armaroli, N.; Barigelletti, F.; Pope, S. J. A.; Ward, M. D. *Inorg. Chem.* **2002**, *41*, 6711. (c) Fletcher, N. C.; Ward, M. D.; Encinas, S.; Armaroli, N.; Flamigni, L.; Barigelletti, F. *Chem. Commun.* **1999**, 2089.

(19) Molecular mechanics calculations have been performed using the SPARTAN02 Computational Suite.

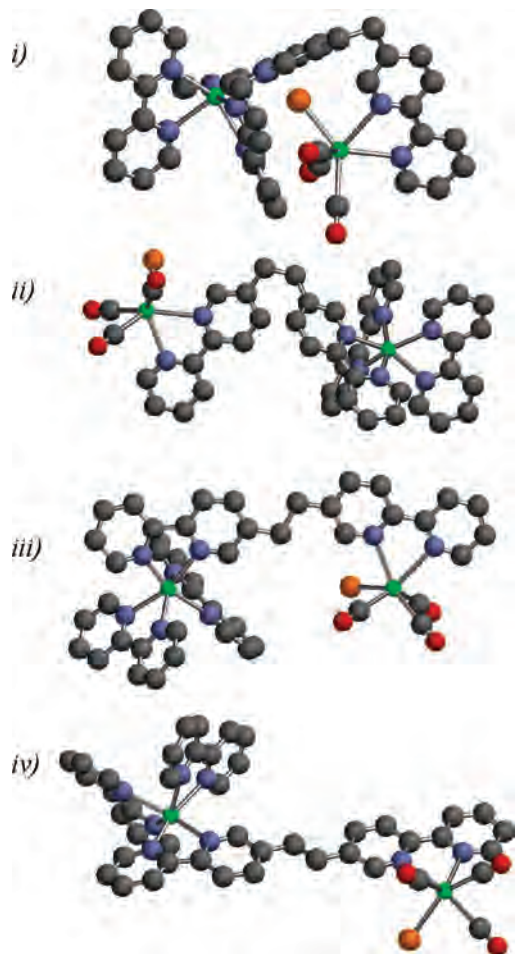


Figure 10. Four possible conformers of **ReLRe** calculated in the gas phase using SPARTAN molecular mechanics package. Amide groups and H atoms were omitted for clarity. See the Supporting Information for further information.

transfer to the Ru \rightarrow L $^3\text{MLCT}$ state. There is some evidence that this is the case in the continued presence of the higher-energy $\nu(\text{CO})_{\text{amide}}$ transient band in the picosecond-TRIR spectra over ca. 1 ns with little appreciable decay observed. This could be caused by the presence of simultaneous energy transfer from the Re \rightarrow L $^3\text{MLCT}$ state and decay of the Ru \rightarrow L $^3\text{MLCT}$ state, both on a time scale of ca. 1 ns. This indicates that the observed process with $\tau = 22 (\pm 10)$ ps could be the faster component, with a slower energy-transfer process in a less compact conformer occurring on a time scale that coincidentally overlaps with the ca. 1 ns decay process, which generates the Ru \rightarrow bpyam $^3\text{MLCT}$ state in the more compact conformer. Given that in other Re^I/Ru^{II} dyads with short saturated spacers the Re \rightarrow Ru energy-transfer process takes place on a time scale of nanoseconds,^{11a,b} this is entirely possible, and research on this multistep energy-transfer process is ongoing.

It should also be noted that the 13 ns energy-transfer process between the Re \rightarrow L $^3\text{MLCT}$ state and the Ru \rightarrow bpyam $^3\text{MLCT}$ state may occur either directly between the chromophores, or via a 13 ns Re \rightarrow L to Ru \rightarrow L energy transfer followed by a rapid (~ 1 ns) decay to the lowest-energy Ru \rightarrow bpyam $^3\text{MLCT}$ state. The data we have recorded cannot distinguish between these two possibilities.

Table 2. Calculated Energy-Transfer Distances Assuming Förster Energy Transfer^a

Re \rightarrow L lifetime ^a	energy-transfer rate (s^{-1})	calcd Förster energy-transfer distance, r (Å)
22 ps	4.54×10^{10}	3.2
830 ps	1.18×10^9	5.9
1 ns	9.68×10^8	6.1
13 ns	4.47×10^7	10.2

^a Measured from TRIR spectra of the $\nu(\text{CO})_{\text{Re}}$ bands in CH_3CN .

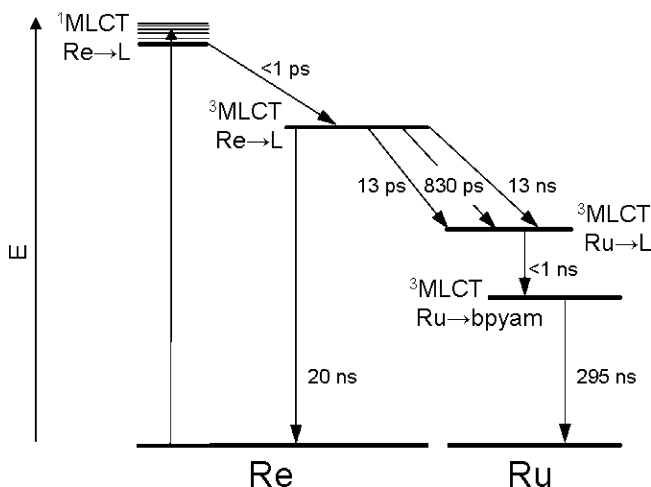


Figure 11. Energy-transfer scheme shown for three primary conformers in solution resulting in three different Re \rightarrow L to Ru \rightarrow L energy-transfer rates.

If it is a two-step process, then this provides evidence for a third conformer in which the Re \rightarrow L $^3\text{MLCT}$ state to Ru \rightarrow L $^3\text{MLCT}$ distance is greater still than either proposed conformation above.

Table 2 reports the calculated distances assuming Förster energy transfer for the four observed energy-transfer rates (see the Supporting Information for details of the calculations). The calculated Förster energy-transfer rates are consistent with at least two major conformers in solution, each of which has two energy-transfer processes, i.e., two Re \rightarrow L $^3\text{MLCT}$ state to Ru \rightarrow L $^3\text{MLCT}$ state energy-transfer processes, over ca. 3 and 6 Å, and two Re \rightarrow L $^3\text{MLCT}$ state to Ru \rightarrow bpyam $^3\text{MLCT}$ state energy-transfer processes, over ca. 6 and 10 Å. As stated above, the very slow (13 ns) energy-transfer process could be evidence for a third conformer if it occurs in two steps, or may occur in a single step. Three of these distances are within the calculated *internuclear* separation range of 5.5–12.6 Å, but, of course, this range is only a guideline to the true distance between the excited states, which are delocalized across both relevant metal and associated ligand. The 22 ps energy-transfer step (corresponding to a rate of $4.5 \times 10^{10} \text{ s}^{-1}$) can only be Förster energy-transfer if the inter-chromophore separation is 3.2 Å, which is less than the smallest metal-metal distance calculated by molecular mechanics (Fig. 10). This process may therefore be occurring by Dexter energy-transfer in a folded conformation, in which overlap of aromatic ligands attached to the different metals provides the necessary electronic coupling. On the basis of these data, more than one possible energy-transfer scheme may be drawn depending on the number of primary conformers that are

present in these experiments. Figure 11 shows a scheme based upon a three-conformation model, in which the $\text{Re} \rightarrow \text{L}^3\text{MLCT}$ state to $\text{Ru} \rightarrow \text{L}^3\text{MLCT}$ state distance varies with the conformation, and the internal Ru-based energy transfer is fixed. It is possible that one or both of the slower energy transfers of ca. 1 and 13 ns may go directly from the $\text{Re} \rightarrow \text{L}^3\text{MLCT}$ state to the $\text{Ru} \rightarrow \text{bpyam}^3\text{MLCT}$ state instead, and this will be the subject of further studies.

Conclusions

TRIR studies on **RuLRe** have provided a much more detailed picture of the $\text{Re} \rightarrow \text{Ru}$ energy-transfer processes than could be obtained from luminescence measurements alone. While the occurrence of energy transfer is obvious from the luminescence behavior, only one component (≈ 1 ns) was unambiguously clear from the rise time of sensitized Ru-based emission. From TRIR data, however, at least three $\text{Re} \rightarrow \text{Ru}$ energy-transfer processes could be identified with lifetimes of ca. 13 ps and 1 and 13 ns. Such complex behavior occurs because of a combination of two different Ru-based $^3\text{MLCT}$ states ($\text{Ru} \rightarrow \text{L}$ and $\text{Ru} \rightarrow \text{bpyam}$), which are sensitized at different rates, and the presence of at least two conformers of the flexible molecule **RuLRe**, which have different $\text{Re} \cdots \text{Ru}$ separations.

Experimental Section

The mononuclear complex $[\text{Ru}(\text{bpyam})_2\text{L}]\text{Cl}_2$ (**RuL**) was available from previous work.¹⁴ Conversion to **RuLRe** was achieved by the reaction of **RuL** (100 mg, 0.08 mmol) with $[\text{Re}(\text{CO})_5\text{Cl}]$ (33 mg, 0.09 mmol) in MeOH/toluene (1:1, v/v)

at reflux for 1 week, affording a red precipitate and a green solution. After evaporation of solvents, the product was purified by preparative TLC on an alumina plate eluting with $\text{CH}_2\text{Cl}_2/\text{MeOH}$ (94:6, v/v). The main orange band was separated and the product removed from the alumina by washing with CH_2Cl_2 to yield the product as an orange powder (30 mg, 24%). IR (solid state): $\nu(\text{CO})_{\text{Re}}$ 2015(s), 1905(m), 1878(s) cm^{-1} ; $\nu(\text{CO})_{\text{amide}}$ 1621 cm^{-1} . IR (CH_3CN solution): $\nu(\text{CO})_{\text{Re}}$ 2024, 1916, and 1898 cm^{-1} ; $\nu(\text{CO})_{\text{amide}}$ 1636 cm^{-1} . MALDI-MS: m/z 1706 $[\text{M} + \text{matrix}]^+$, 1483 $[\text{M} - 2\text{Cl} - \text{H}]^+$ (matrix is 3-nitrobenzyl alcohol). Calcd for $[(\text{bpyam})_2\text{Ru}(\text{BL1})\text{Re}(\text{CO})_3\text{Cl}]\text{Cl}_2 \cdot 3\text{H}_2\text{O}$: C, 50.07; H, 5.02; N, 10.46. Found: C, 49.98; H, 5.26; N, 10.04. The NMR spectrum was broad and uninformative, probably because of the presence of slowly interconverting conformers.

Details of the equipment and methods used for the luminescence and TRIR studies have been described previously.^{9,20} TRIR spectra are shown with ca. 4 cm^{-1} resolution, and data have been fitted using a spline function.

Acknowledgment. We thank the EPSRC for financial support (Grants GR/S50724 and GR/S50731). We thank the Science and Technology Facilities Council for access to the Central Laser Facility.

Supporting Information Available: Förster energy-transfer and molecular mechanics calculations. This material is available free of charge via the Internet at <http://pubs.acs.org>.

IC702005W

(20) Towrie, M.; Grills, D. C.; Dyer, J.; Weinstein, J. A.; Matousek, P.; Barton, R.; Bailey, P. D.; Subramaniam, N.; Kwok, W. M.; Ma, C.; Phillips, D.; Parker, A. W.; George, M. W. *Appl. Spectrosc.* **2003**, *57*, 367.